ELSEVIER

International Journal of Heat and Fluid Flow 20 (1999) 530–537

International Journal of HEAT AND FLUID FLOW

www.elsevier.com/locate/ijhff

Analysis of the spray forming process using backscattering phase-Doppler anemometry

Jörg Tillwick *, Volker Uhlenwinkel, Klaus Bauckhage

Department of Chemical Engineering, University of Bremen, SFB372, Badgasteiner Straße 3, 28359 Bremen, Germany

Abstract

A phase-Doppler anemometer (PDA) was extended for the analysis of metal melt gas-atomization. Because of the optical properties of liquid or partly solidified spherical particles with a high value of the imaginary part of the refractive index (which means that measurements can be executed, using the reflected light from the particles), the instrument was arranged in a 180° backscattering position, with a combined transmitting and receiving system. This compact assembly described in principle already by Bauckhage in 1988 and 1989 can easily be moved to realize different measuring locations in the spray cone, needing only one window. Operating from one side of the spray cone scanning PDA-measuring positions from inside the two phase flow could be carried out within milliseconds per measuring position, thus allowing the analysis even for short atomization duration. Due to high particle rates in the spray cone and a difficult optical behavior of the solidified metal particles (rough surface), a new signal processing had to be developed, which can be subdivided into a signal recording and a post processing. During the first part a signal is completely recorded for a definite duration without using any trigger criteria. This results in a kind of signal band, that contains bursts as well as noise. In the second part the bursts are removed from the signal band by using the signals power spectrum after a fast-Fourier transformation (FFT). © 1999 Elsevier Science Inc. All rights reserved.

Keywords: Phase-Doppler anemometry; Spray forming; Signal processing

Notation

d	particle diameter
Δd_z	axial size of measuring volume
f	focal length
FFT	fast-Fourier transformation
L1/L2	lenses (beam expansion)
L3/L4	lenses (sending-receiving system)
M1/M2	mirrors
$\dot{M}_G$	atomization gas flow
$\dot{M}_L$	metal melt flow
MV	measuring volume
r	radial distance in spray cone
R1/R2	receiver
RDG	radial diffraction grating
SNR	signal-noise-ratio
TL	trigger level
v	particle velocity
Δz	interference fringe spacing
z	axial distance in spray cone
$\theta/2$	half beam crossing angle
λ	laser wave length
Ψ	elevation angle
φ	off-axis angle

1. Introduction

During spray forming, a continuous stream of liquid metal is atomized by inert gas, forming a spray of melt droplets with a size range between 5 and 500 μm in diameter (Singer, 1970, 1972; Grant 1995). These particles are accelerated towards a substrate where they impinge and consolidate to build up a solid pre-form (deposit). Due to hostile environmental conditions inside the atomization chamber, a non-intrusive measurement method must be used for the analysis of the spray forming process. In the case of spherical particles, as produced by the liquid metal gas-atomization, PDA appears to be an appropriate tool enabling not only the characterization of the particle size and velocity distribution but also additional information as for instance the determination of local mass flux distributions and in combination with additional information the calculation of the enthalpy input into the deposit. For process modeling further information about the size, the relative velocity of the particles and about the local dependence of the cooling conditions of the particles are needed. The local particle velocity, in connection with the particle diameter, leads to its impulse. If both quantities are received from a location near the surface of the deposit, the impulse at impact can be concluded.

Goal of the present investigations was to adapt the PDA technique to the process of molten metal atomization in general. Since standard phase-Doppler systems can easily be applied to conventional materials, e.g., small water droplets or

* Corresponding author. E-mail: till@iwt.uni-bremen.de

PII: S0142-727X(99)00042-9

highly reflecting, solid metal spheres with smooth surfaces, the optical behavior of the solidifying particles in this process depends strongly on their surface structure, i.e., on their temperature and on their status of solidification. Therefore, an extension of the PDA technique was necessary.

2. Spray forming – process description

Typical spray formed materials are, for example, copper and copper alloys, (low carbon) steel, aluminium, aluminium alloys or tin. The present investigations are carried out using copper. The metal is melted in a crucible by an inductive heater with a superheat of 50–300 K. The melt is poured into a heated tundish (Fig. 1) with an outlet diameter of 4–5 mm. Generally the ambient atmosphere in the melting vessel and in the spray chamber is nitrogen, which is also used as atomization gas. The atomizer is located below the outlet of the tundish. Both, close coupled and free fall atomizers can be used for the process. Before atomization takes place in the latter atomizer the melt forms a liquid jet falling a short distance in an undisturbed manner. Then it is atomized by high velocity gas jets into a spray of molten droplets. These are accelerated downwards towards a substrate where they impinge and consolidate to become a solid pre-form (the deposit) of a typical shape, for instance billet, tube or plate.

The spray forming process is controlled by different process parameters. One of these and the most important is the atomization gas mass flow and its relation to the melt mass flow ratio: GMR). For the present investigations only this GMR has been varied, as shown in Table 1, by keeping the melt mass flow constant and changing the atomization gas mass flow. Thus, two GMR's of 0.95 and 1.345 have been realized.

3. Experimental set-up

On-line particle size and velocity measurements by PDA during spray compacting processes were first introduced by Bauckhage and coworkers (see, e.g., Bauckhage, 1988; Bauckhage and Schreckenberg, 1989; Bauckhage et al., 1989).

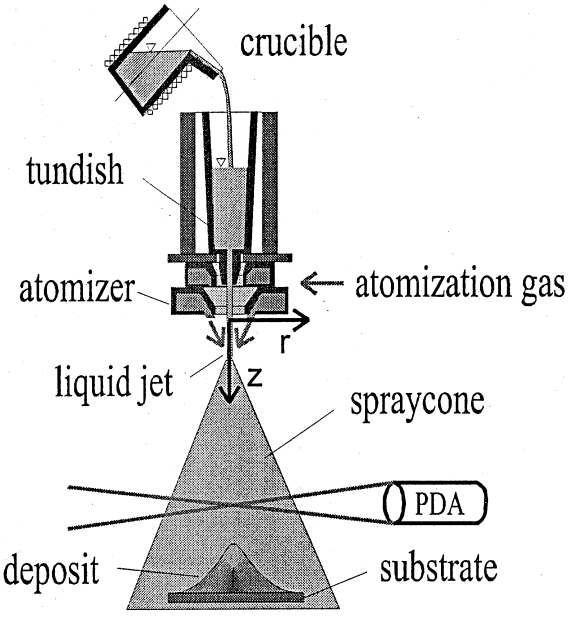

Fig. 1. Principle of spray forming plant.

Table 1
Process parameters of atomization experiments

Type of atomizer	Free fall atomizer
Atomization gas	Nitrogen
Gas flow: $\dot{M}_G$	(a) 0.206 kg/s and (b) 0.292 kg/s
Melt flow: $\dot{M}_L$	0.195 kg/s
Material	Copper
Melt super heat	300 K
Melting temperature	1083°C

Generally, it was shown in this investigation that the determination of particle size and velocity distribution is possible. However, as pointed out by Liu et al. (1990) and Heuermann et al. (1992) the application is limited by the tendency of the metal droplets to form typical surface structures during the individual solidification process. These structures depend on the material properties of the melt, on the particle size and on the very special cooling conditions. While large particles remain liquid for a longer time, small particles tend to solidify rapidly. When solidification starts, the crystallization, starting from the particle surface, tends to form dendritic structures, and the surface turns from smooth to rough. This leads to weak and noisy signals, because parts of the incident laser light are scattered arbitrarily from the rough particle surface.

Thus the distance of the axial measuring position below the atomizer exerts a strong effect on the signal quality, because more and more particles solidify due to an increasing flight duration and cooling time after atomization. Consequently, with decreasing particle size and increasing distance from the atomizer, growing numbers of particles get rough surfaces, thus influencing the signal quality which becomes worse.

Further problems occur from high particle rates (dense spray) and a growing dust content in the spray chamber, both leading to an increasing attenuation of the incident laser beams and the reflected light from the particles. An increasing attenuation of the laser light inside the spray chamber is one reason for an underestimation of smaller particles, as pointed out already for example by Farmer (1976), Yule et al. (1977), Schöne (1993) or Roberds et al. (1979). Generally, small droplets deliver low signal intensity and therefore, under these conditions, low signal-to-noise ratio (SNR).

The problems mentioned result from the atomization process itself. A further major problem for signal receiving occurs from the short atomization duration (a limitation due to the present spray forming plant). Due to a restricted melt reservoir, constant atomization conditions can only be realized for approximately 100 s. During this time up to seven PDA runs have to be carried out. For each PDA-measurement run the PDA-measurement volume shall be moved to different positions in the spray cone. As will be shown, the PDA was prepared in a certain way to overcome the problems mentioned.

3.1. Implementation of PDA setup

As can be seen from Fig. 2 the phase-differences $\Delta\Phi$ (of the reflected light) versus off-axis angle φ show for $\varphi = 180°$ a linear dependency from the copper particle diameter d, which gives rise for the use of a simple $\Delta\Phi(d)$ relationship. Therefore the reflected light of molten or ideal solidified metal droplets can be used for phase-Doppler measurements for nearly all off axis angles φ apart from near forward diffracted light. Hence, the PDA experimental setup was arranged in direct backscattering direction ($\varphi = 180°$) which was most promising for the present measuring task for several reasons. As shown in Fig. 3, the sending and receiving systems are mounted on the same chassis using partly the same optics. Beam expansion (L1/L2),

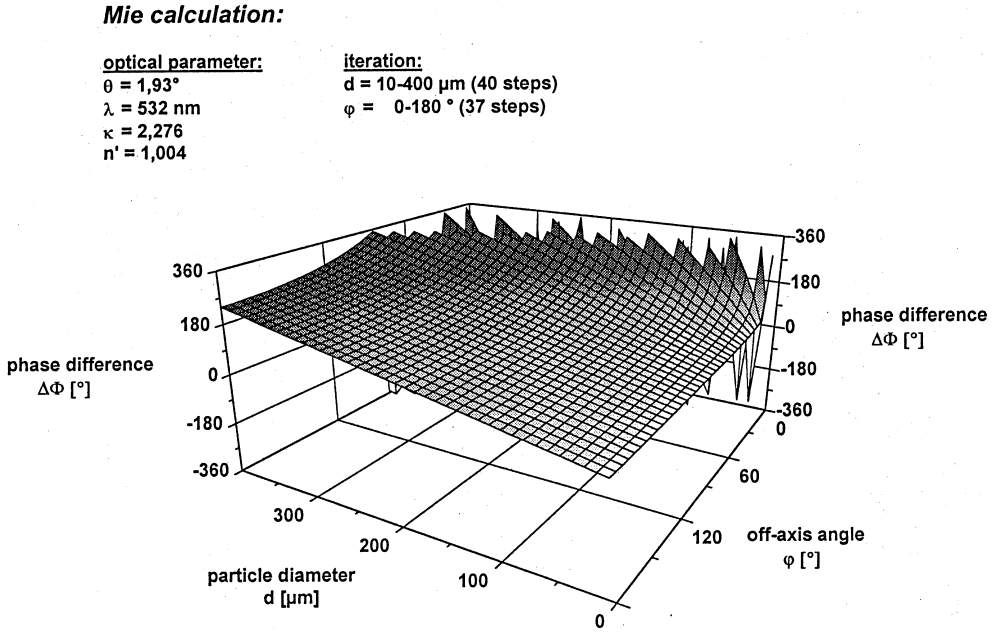

Fig. 2. Mie calculations for copper particles; particle diameter d (<400 μm) vs. off-axis angle φ show linear dependency $\Delta\Phi(d)$ for $\varphi = 180°$.

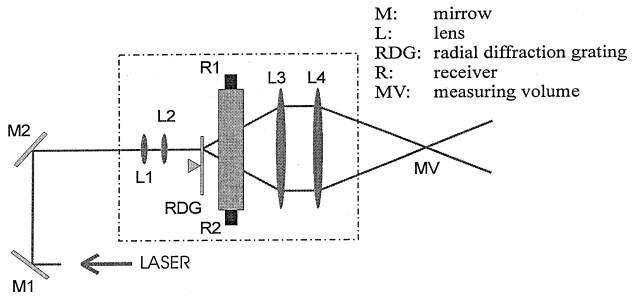

Fig. 3. Scheme of coupled sending–receiving system of PDA assembly (backscattering arrangement).

beam separation (RDG), both receivers (R1/R2) and the sending-receiving lens L4 are arranged in one common body. This guarantees a compact assembly that is easily to adjust. The measuring volume thus can be moved in vertical and horizontal directions by using a bare-type pick-up base. Hence, different measuring locations in the axial and radial direction, relating to the spray cone, can be examined. In order to reduce weight and to minimize the dimensions of the assembly, the sending–receiving system was decoupled from the LASER by using two mirrors (M1/M2). Further specifications due to the PDA experimental setup are given in Table 2.

Table 2
Data of PDA-experimental setup

Data of the PDA-setup (backscattering arrangement)	
Wave length: λ	532 nm
Off-axis angle: φ	180°
Focal length (L4): f	990 nm
Half beam crosing angle: $\theta/2$	0.96°
Elevation angle: Ψ	2.65°
Interference fringe spacing: Δz	15.81 μm
Size of the measurement volume	
Δd_z: (in direction of main particle movement)	648 μm
Measuring range	
Maximum particle diameter: d_{max}	683 μm
Maximum particle velocity: v_{max}	316 m/s
Measuring location	
Axial (distance from nozzle): z	150 . . . 565 mm
Radial (position in spray cone): r	0 . . . 60 mm

3.2. Signal processing

As mentioned above, signal processing has to overcome some serious problems due to this type of atomization process. These are a short spray run duration and a poor signal quality. The time-consuming part of signal processing is the evaluation of the received data. To reduce the over all measuring time, signal processing was subdivided into *signal recording* and *post processing* (*evaluation*).

3.2.1. Signal recording

The aim of signal recording is to realize short PDA measuring duration, to accommodate to the short spray run duration, while getting a high amount of particle counts at the same time. In general PDA-bursts are detected by setting trigger criteria, as described for example by Schöne (1993), Flögel (1987), Ruck (1987), Maeda et al. (1988) or Macloed (1985), to remove the bursts from the noise. Often the bursts amplitude is used as trigger criteria. This requires almost ideal measuring conditions, which for instance can be found from water droplets using droplet generator experiments. The diagram at the top in Fig. 4 represents the amplitude spectrum of a burst with high signal-to-noise ratio (SNR), taken from such a water droplet of a mono disperse spray. The bursts amplitude, represented by the left ordinate, is much higher than that of the surrounding noise. Hence, the burst emerges clearly above the noise and can be removed easily from the signal band by using the amplitude spectrum. However, ideal measuring conditions like these are not usual with metal melt atomization. The diagram at the bottom represents the amplitude spectrum of a burst with low signal-to-noise ratio, which is typical for metal melt droplets from the spray forming

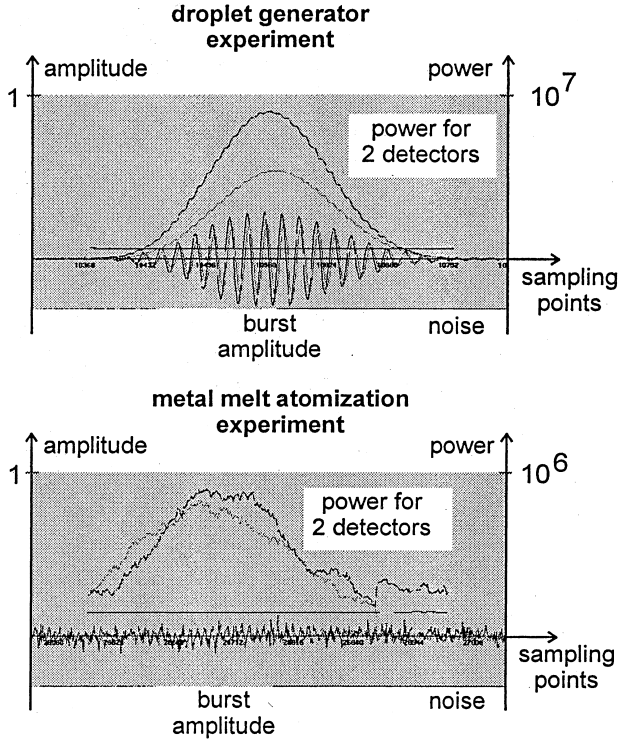

Fig. 4. Part of a signal band of extended PDA signal processing; burst and noise amplitude spectrum, power level after fast-Fourier transformation for two PDA detectors.

process. The burst's amplitude is almost of the magnitude of the noise and below, respectively. Therefore it is vanishing into the noise level. Hence, this burst can't be removed from the signal band by using the burst amplitude. Further information is needed for the detection of this burst, which can be received by a FFT, as will be discussed below.

In order to realize a fast signal recording with a high particle rate, signal is completely recorded for a definite time, first without using any trigger criteria. Hence, a kind of *signal band* is recorded that includes bursts as well as noise. This signal band is stored to a hard disk, without any data evaluation. By using this signal recording method, the time for a PDA-measurement run can be reduced to less than 1 s. The storage duration takes about 15 s, but this time is not wasted. It can be used for moving the PDA experimental setup, in order to realize one of the next different measuring locations. After storing, the system is ready for the next measurement. Dependent on the local particle rate in the spray cone, the signal band might contain up to 10^5 bursts. If the number of bursts at the measuring position should be insufficient (in a statistical sense) the measuring duration can be extended.

3.2.2. Post processing

After this fast signal recording, the bursts have to be removed from the signal band by using the post processing procedure. Because no time limits exist for the evaluation at this point, different trigger and/or evaluation criteria can be used in order to handle the poor signal quality. As mentioned above, due to poor signal quality, further information is required for burst detection. This information comes from a FFT of the signal band. The FFT delivers not only the frequency of a signal, but also its power. The phenomenon used here is, that the power of pure white noise spreads over a wide range, because it consists of random frequencies, whereas the power of a burst is mainly represented by just one frequency.

A FFT is used for each sampling point of the signal band (the sampling points are represented by the abscissa of both diagrams), each step covering a *window* of 128 sampling points. The first sampling point for which a FFT can be used is the 64th, in order to have this point in the middle of the 128-points-window that is under investigation. After evaluating the power level at this point, the 'FFT-window' is shifted one sampling point ahead. Again a 128 points FFT is executed, beginning 64 points before and stopping 64 points behind this new, momentary investigated sampling point. In this manner the FFT is used for each sampling point of the signal band.

The evaluated values of the power level of each sampling point are represented by the two Gaussian like curves of both diagrams in Fig. 4, dependent on the two receivers of the PDA experimental setup. The curves are related to the right ordinates of the diagrams. It has to be mentioned, that both right ordinates do not have the same level. The level of the one at the top is in the magnitude of 10^7, whereas the level of the lower diagram is only in the range of 10^6. Nevertheless, it can be seen clearly, that in both cases, whether good or poor signal quality occurs, the power level represented by a burst is much higher than the average power level of the noise.

For burst detection a trigger level is enabled in this power level range. When the power rises above the given power trigger level, a burst has to be expected. Starting at this sampling point, a 128 sampling points window is cut off the signal band, but the trigger is not enabled again at this time. First of all this window is stored to a data file, which includes all windows that were found within the signal band. To avoid multiple particle counts, resulting from Doppler signals consisting of more than 128 sampling points, the end of the Doppler signal has to be detected. This is guaranteed by enabling a second trigger level at the trailing edge of the power signal. Until the power level is not falling below this second final trigger level, the first (incoming) trigger level will not be enabled again, and therefore no further Doppler signal can be detected. By reducing the power trigger level to a value barely above the power level of the noise, the total amount of particle counts increases. This especially holds for small particles with low signal power.

After finding and extracting the bursts from the signal band, further evaluation criteria can be used with the bursts being now stored in the data file. The acceptance rate of detected to evaluated bursts is about 80%. Because the raw signal (bursts and noise) is stored to a hard disk, it is possible to evaluate the data again and again using different trigger and evaluation criteria for each rerun.

3.3. Atomization process conditions and parameters

In order to verify the general applicability of the extended experimental PDA setup and the new signal processing during molten metal atomization, sensitivity tests and measurements were performed during several spray forming experiments under different process conditions. The spray cone may be considered to be axisymetric to its center line, Uhlenwinkel (1992), Brooks et al (1980) Grant (1995). Hence, for a fixed axial distance from the atomizer, PDA measurements have to be carried out only along a radial line in order to receive information about the cross section of the spray cone at different axial distances from the atomizer. At each axial distance at least six radial measurements were carried out for a fixed atomization gas-to-melt mass flow ratio, starting at the center line of the spray cone ($r = 0$ mm), and increasing the radial distance for each further measurement. Thus, radial positions between 40 and 60 mm, dependent on the radial dimensions of the spray cone, could be realized, and one is able to characterize the cross area of the spray cone at this fixed axial

distance by just a few (5–6) measurements. The last measurement was always readjusted to the center line, which delivered in general the reference measurement for all measurements of one plain. This confirmed the assumption of stationarity of the spray conditions. Since stationary atomization conditions can be assumed for all measuring positions, all radial measurements are performed during a single atomization run.

For the present investigations a raster of measuring positions was scanned in axial and radial direction of the spray cone. PDA-measuring volumes were positioned at five different axial distances below the atomizer. The values for the minimal and maximal axial distances from the atomizer are limited by the dimensions of the chamber window, through which the atomization process is examined by PDA.

4. Results and discussion

Several PDA-measurements were carried out during different metal melt atomization experiments. In this context we used a pure (unalloyed) copper melt. The atomization gas was nitrogen, its gas-to-melt mass flow ratio was varied as given in Table 1.

In Fig. 5 the change of the gas-to-melt mass flow can be recognized by its effect on particle size and mean velocity. Both measurements were taken at a fixed position on the centerline of the spray cone at an axial distance of 500 mm below the atomizer for different atomization conditions. The number density distribution, represented by the left ordinate, and the mean particle velocity per size class, represented by the right ordinate, are given for a particle size range up to 500 μm. The lower gas mass flow is represented by filled squares for the number density distribution, and blank squares for the mean particle velocity per size class, whereas the higher gas mass flow is represented by filled and blank circles. One can see, that the number density distribution for the higher gas mass flow is shifted to smaller particle diameters, and it is a more narrow distribution. The shift to smaller size classes is characterized for example by the peak value of the distribution, that occurs left from that for the distribution of the lower gas mass flow rate. Looking at the particle size classes one can see from the particle velocity (in z-direction), that the absolute particle velocity is much higher in case of the higher gas flow. This ranges between 20 m/s for particle diameters of 150–200 μm and rises up to 30–40 m/s for smaller particles of 50–100 μm. Both, decreasing particle diameter and increasing mean velocity are plausible for an increasing atomization gas flow with the present atomization process.

Also the velocity–diameter (v–d) correlation for all measurement results is plausible with the present atomization process characteristic. In Fig. 6 this correlation is shown exemplary for the high gas mass flow and for one measuring position ($z = 500$ mm, $r = 0$ mm). The correlation of particle velocity and diameter represents absolute values for both quantities of the evaluated signals. In this case the particles are not classified by different particles size classes, and also the corresponding velocity is not a mean value, but the momentary velocity of an individual particle. Therefore the v–d correlation results in a cloud of measuring points, each representing a particle of definite diameter and velocity.

It has to be observed, that, due to the local gas velocity in z-direction, in general smaller particles have a higher local velocity in z-direction compared with the larger particles. This corresponds with theory, as described for example by Liu (1990) and Kramer (1997). Corresponding to the local velocity difference to the atomization gas velocity, the particles are accelerated at first (for small axial distances). This acceleration affects smaller particles much more due to their smaller mass and inertia. Therefore particles of smaller diameter are in general much faster than larger particles for small axial dis-

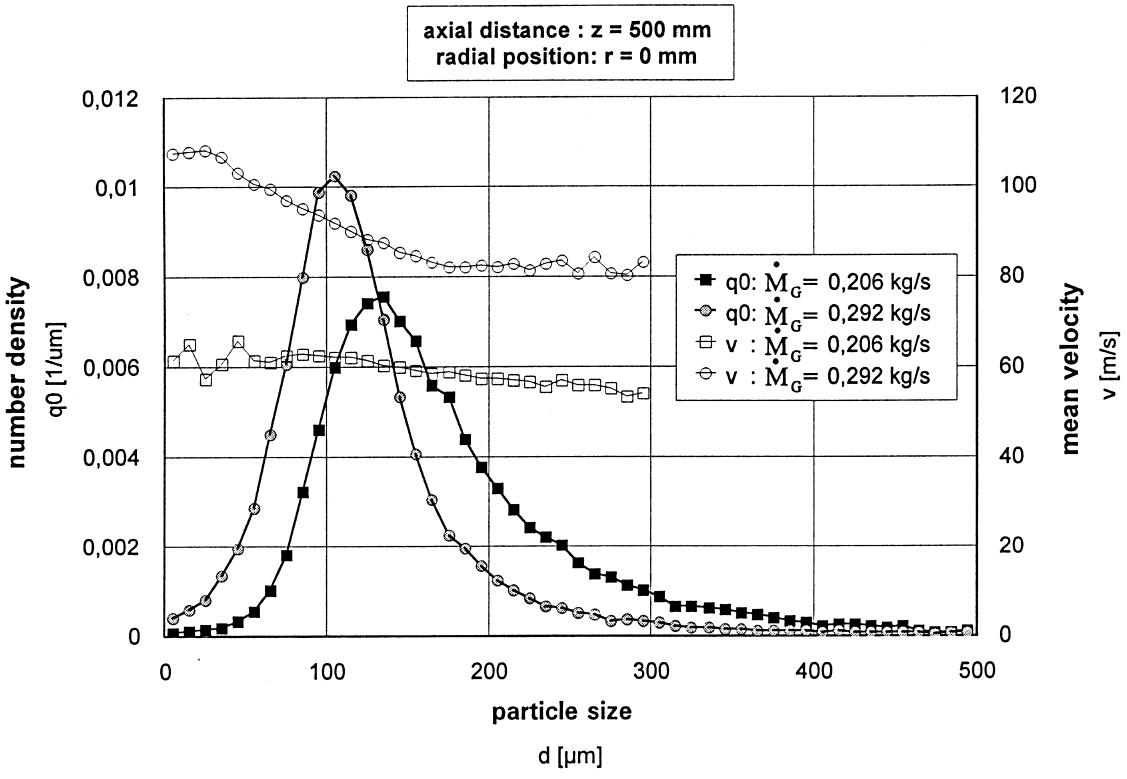

Fig. 5. Number density distribution and mean particle size class velocity for a fixed measuring position, dependent on different gas flow rates.

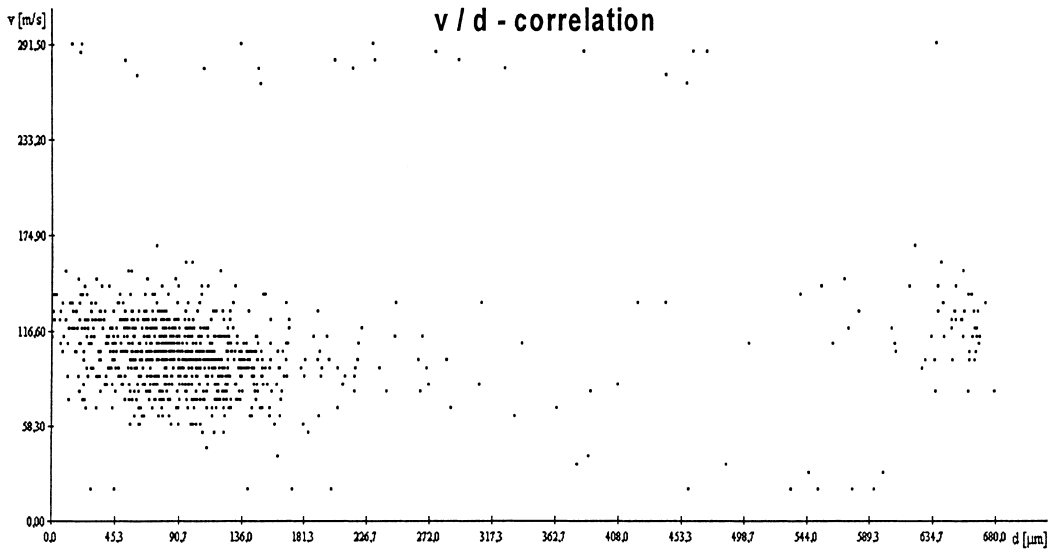

Fig. 6. Velocity–diameter (v–d) correlation for the high gas flow (compare Fig. 5).

tances. In the course of time, with increasing flight duration, the particle velocity approaches the gas velocity. From this point, the particles are decelerated, because the gas velocity decreases for growing axial distances from the atomizer. During this time the particle velocity is higher than the gas velocity, due to inertia of the particles. The behavior of particle velocity, dependent on particle size and axial distance from the atomizer could be recognized by PDA-measurements, which are discussed below in more detail.

Fig. 7 shows results of the mean particle velocity per size class, depending on the axial measuring position in the spray cone. Results are given for three different particle size classes: 50, 100 and 150 μm. The measurements were carried out on the center line of the spray cone, for the lower atomization gas mass flow ($\dot{M}_G = 0.206$ kg/s). Independent of the particle size, at first an increase in mean particle velocity can to be observed for increasing axial distances. For axial distances above 500 mm, velocity begins to decrease for particles of 50 μm (and smaller), while no remarkable change can be seen for the 100 μm particle. Particles of 150 μm (and above) experience a further increase in velocity due to their inertia. The reasons were given above. Again the smallest particle size class shows the highest absolute mean velocity of the three size classes.

Fig. 8 shows results of mean particle velocity per size class, dependent on the radial measuring position in the spray cone. Results are given for three different particle size classes: 50, 100 and 150 μm. The measurements were carried out at an axial distance of $z = 380$ mm (below the atomizer) for the higher gas mass flow rate. In general only a slight increase in mean velocity is to be observed for all three size classes up to a radial distance from the center line of 45 mm. For all radial positions the smallest size class shows the highest absolute velocity. For radial positions above 45 mm a decrease in velocity is to be observed independent of the particle size. This can be explained by exchange processes between the spray cone and the ambient atmosphere in the spray chamber. Hence, for the presented axial position below the atomizer, the edge of the spray cone can be given for radial positions above 45 mm.

Fig. 9 shows a comparison between PDA-measured and computed results for the gas and particle velocity due to different particle sizes versus the flight distance z (from the point of atomization). The results are given for the centerline of the spray cone, for the higher gas flow ($\dot{M}_G = 0.292$ kg/s). The simulation (computed values) shows a strong acceleration of the smaller particles (10 and 30 μm in diameter) and moderate

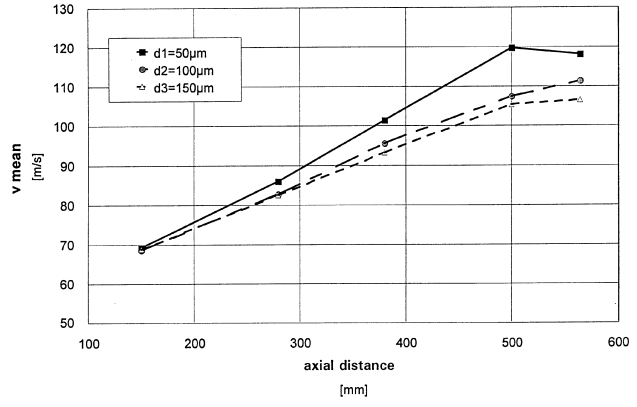

Fig. 7. Mean particle velocity for three different particle size classes, dependent on axial distance from the atomizer.

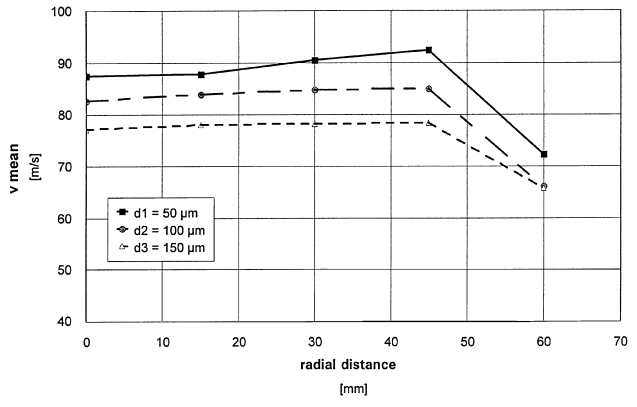

Fig. 8. Mean particle velocity for three particle size classes, dependent on radial position in the spray cone.

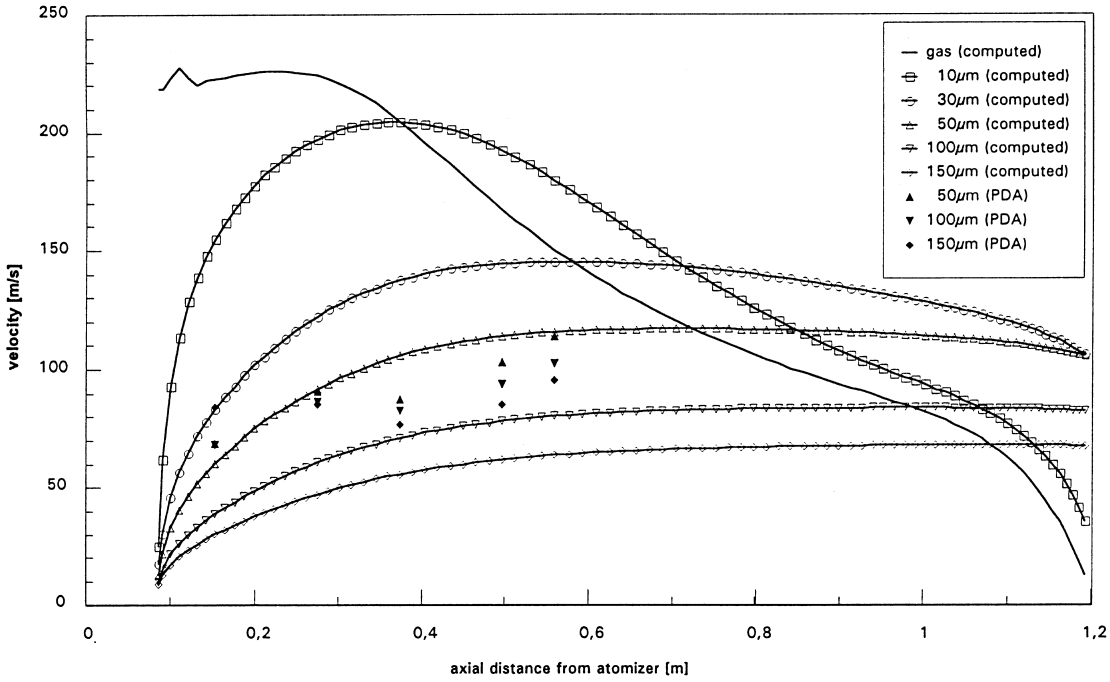

Fig. 9. Comparison between PDA-measured and computed results for gas and particle velocity for different particle sizes vs. flight distance from the point of atomization (for the centerline of the spray cone); computed values by Bergmann (1998).

ones (with growing velocity values till $z \geqslant 700$ mm) of the larger particles (50, 100, 150 μm in diameter). This situation is typical for the multi phase flow of the spray forming process, as already discussed above. Since the computed and the measured results for $d = 50$ μm are in excellent agreement, also in most other cases the tendency of the computed results is confirmed by the measured ones quite well. Only in the region nearer to the atomizer ($z \leqslant 150$ mm), i.e. in the high density region, both results differ from each other, what seems to be tolerable as well as for the simulation program as for the measuring technique. In the dense spray region primary atomization and further droplet disruption as well as droplet collision and agglomeration take place. This dense spray region seems to turn over into the more dilute region at distances z of about 200 mm, where droplet–droplet interaction is no longer significant. From here spray cone modeling becomes successful since droplets motion can be regarded either as an isolated process with its individual drag coefficient and heat transfer parameters or as adequate numerical mode depending on its capability to include coupling effects between the particulate and the carrier phase (Crowe, 1997). A one way coupled model would account for the effect of the flow field on the droplet motion and thermal properties but would not include the effect of the droplets on their carrier phase. A fully coupled model includes interactive effects of both phases. The coupling is especially important because of the estimation of the differing heat transfer rates between the melt particles (with various diameters) on their different paths to the deposit and the variations of heating up the gas stream either in the center or at the outer regions of the spray cone.

Though there has been reported considerable work in this area, measuring techniques so far have remained as off-line techniques, thus forcing the interpretation of process results to deduce the relevant theories from ex-post analyses. The aim of our research works is to develop the PDA not only as an in-line technique, but also as an on-line technique, which, together with ex-post analyses, allows process control.

5. Conclusion

The aim of the present work was the adaptation of an extended PDA setup to the atomization process of molten metals. Problems occurring by the application of PDA to this process have been presented. These problems result from the particle size dependent particle surface structure, due to particle cooling and solidification/crystallization, high particle rates and high dust content, and short atomization duration. All of these are typical for the spray forming process, and the plant scale of the present spray forming plant, respectively.

To realize measurements at different locations in the spray cone inside the hostile atmosphere of the spray chamber, a moveable PDA assembly was developed in a backscattering arrangement. To handle poor signal quality, and to get a fast data recording, a new signal processing software was developed. This can be subdivided into (a) signal recording and (b) post processing.

Results were presented for different radial and axial measuring locations. During these measurements, one of the most important atomization process parameters – the atomization gas mass flow – was varied. It could be shown, that a decrease in particle size and an increase in particle velocity, corresponding to an increasing atomization gas mass flow, can be well recognized. An increase (and later decrease) of particle velocity can also be obtained for growing axial distance from the atomizer, while radial dependencies for fixed particle sizes could be neglected. These results indicate the boundaries for the PDA-measuring positions within the spray cone in order to use PDA for on-line measurements (process control) and give advice for the limitations of PDA sensitivity with respect to the most important process parameter variations of the GMR.

Also computed and measured results for the gas and particle velocity due to different particle sizes versus the flight distance z showed quite good agreement (for $d = 50$ μm). At least the tendency of the computed results is confirmed by the measured ones quite well in most other cases.

Acknowledgements

The present investigations have been performed at the spray forming plant of the Special Research Project (SFB372-TP A8) at the University of Bremen. The authors gratefully acknowledge the financial support of the Deutsche Forschungsgemeinschaft (DFG).

References

Bauckhage, K, 1988. Applications of the phase-Doppler-method to spray analysis. In: Proceedings of ICLASS'88, Sendai, Japan, pp. 279–286.

Bauckhage, K., Schöne, F., Dopheide, D., 1989. Phase Doppler measurements using laser- and avalanche photo-diodes in a backscattering arrangement. In: International Conference on Laser Anemometry Advances and Applications, Swansea, Wales.

Bauckhage, K., Schreckenberg, P., 1989. Control of power-metal-production; a new application on phase-Doppler-anemometry. In: Proceedings of the International Conference on Mechanics of two-Phase flows, Taipei, Taiwan, pp. 1–6.

Bergmann, D., 1998. Simulation of the multiphase flow of the spray cone at the spray forming process. Personal report, University of Bremen.

Brooks, R.G., Leatham, A.G., Dunstan, G.R., 1980. Osprey technology for spray-deposited preforms and powders in superalloys. In: Proceedings of the Conference on Powder Metallurgy Superalloys.

Crowe, C.T., 1997. Challenges in numerical simulation of metal sprays in spray forming processes, Colloquium in the course of the special research project (SFB372) at the University of Bremen, Colloquium Volume 2, pp. 1–16.

Farmer, W.M., 1976. Sample space for particle size and velocity measuring interferometers. Applied Optics 15, 1984–1989.

Flögel, H.-H., 1987. Modifizierte Laser-Doppler-Anemometrie zur simultanen Bestimmung von Geschwindigkeit und Größe einzelner Partikeln, Dissertation, University of Bremen.

Grant, P.S., 1995. Spray forming. Progress in Materials Science 39, 497–545.

Heuermann, J., Bauckhage, K., Wriedt, T., Schöne, F., 1992. On-line roughness measurement by modified laser-Doppler anemometry for studies of solidification of moving molten metal droplets, Preprint of the European. Symposium on Particle Characterisation, Nürnberg, Germany, pp. 375–390.

Kramer, C., 1997. Die Kompaktierungsrate beim Sprühkompaktieren von Gaußförmigen Deposits, Dissertation, University of Bremen.

Liu, H., Seuren, B., Uhlenwinkel, V., Bauckhage, K., 1990. Spray forming of liquid steel; Local size and velocity distributions of particles in the spray cone and their reference to varying process parameters. In: International Conference on Powder Metallurgy, London, UK.

Liu, H., 1990. Berechnungsmodelle für Geschwindigkeiten und die Abkühlung von Tropfen im Sprühkegel einer Stahl-Zerstäubungsanlage, Dissertation, University of Bremen.

Macloed, M.D., 1985. LDV signal processing with ultra fast DFT processor. In: Proceedings of the Sixth International Conference on Photon Correlation and Other Techniques in Fluid Mechanics, Cambridge.

Maeda, S.N., Kobashi, K., Hishida, K., 1988. Measurement of spray mist flow by a compact fiber LDV and Doppler-shift detector with a fast DSP. In: Proceedings of the Fourth International Symposium on Applications of Laser Anemometry to Fluid Mechanics, Lisbon, Portugal.

Roberds, D.W., Brasier, C.W., Bomar, B.W., 1979. Use of a particle sizing interferometer to study water droplet size distribution. Optics Engineering 18, 236–242.

Ruck, B., 1987. Laser-Doppler-Anemometrie. AT-Fachverlag GmbH, Stuttgart.

Schöne, F., 1993. Wichtung von Partikelgrößenverteilungen in der Phasen-Doppler-Anemometrie, Dissertation, University of Bremen.

Singer, A.R.E., 1970. The principles of spray rolling of metals. Metals and Materials 4, 246–250.

Singer, A.R.E., 1972. Aluminium and aluminium alloy strip produced by spray deposition and rolling. Journal of the Institute of Metals 100, 185–186.

Uhlenwinkel, V., 1992. Zum Ausbreitungsverhalten der Partikeln bei der Sprühkompaktierung von Metallschmelzen, Dissertation, University of Bremen.

Yule, A.J., Chigier, N.A., Atakan, S., Ungut, A., 1977. Particle size and velocity measurements by laser anemometry. Journal of Energy 1, 220–228.